ELSEVIER

Physics Letters B 526 (2002) 315–321

PHYSICS LETTERS B

www.elsevier.com/locate/npe

# Interaction potential between heavy ions

V.Yu. Denisov [a,b]

[a] *GSI, Planckstrasse 1, D-64291 Darmstadt, Germany*

[b] *Institute for Nuclear Research, 03650 Kiev, Ukraine*

Received 5 September 2001; received in revised form 2 November 2001; accepted 27 December 2001

Editor: J.-P. Blaizot

**Abstract**

The semi-microscopic potential between heavy ions is evaluated for various colliding ions in the approach of frozen densities in the framework of the extended Thomas–Fermi approximation with $\hbar^2$ correction terms in the kinetic energy density functional. The proton and neutron densities of each ion are obtained in the Hartree–Fock–Bogoliubov approximation with SkM* parameter set of the Skyrme force. An expression for the ion–ion potential well fits the semi-microscopic potentials in the wide range of both colliding ions and distances between them. © 2002 Elsevier Science B.V. All rights reserved.

*PACS:* 21.10.Dr; 25.70.Jj; 27.90.+b

*Keywords:* Heavy ions potential

## 1. Introduction and summary

Knowledge of the ion–ion interaction potential is a key ingredient in the analysis of nuclear reactions. By using the potential between nuclei we can estimate the cross sections of different nuclear reactions [1–3]. The cross sections of elastic, inelastic and fusion reactions between heavy ions are strongly dependent on the nucleus–nucleus interaction potential [1–3].

The ion–ion interaction potential related to the Coulomb repulsion force and the nuclear attraction force has, as a rule, the barrier and the capture potential well near a touching point. The Coulomb part of the ion–ion potential is well-known. In contrast, the nuclear part of the nucleus–nucleus potential is less defined. There are many different approaches to the nuclear part of the interaction potential [1–8]. Unfortunately, barriers evaluated within different approaches for the same colliding system differ considerably, especially when both nuclei are very heavy or one nucleus is very heavy and another is light. The uncertainty of the interaction potential between heavy ions near the touching point gives rise to a variety of proposed nuclear reaction mechanisms. So, there is a need to reduce the uncertainty of the interaction potential around the touching point.

Below we evaluate the nuclear part of interaction potential between heavy nuclei in the semi-microscopic frozen density approximation due to a short reaction time. The frozen (or sudden) approximation is good for evaluation of the ion–ion potential near the touching point at collision energies above the

*E-mail addresses:* v.denisov@gsi.de, denisov@kinr.kiev.ua (V.Yu. Denisov).

0370-2693/02/$ – see front matter 
PII: S0370-2693(01)01513-1

barrier height. The shape of each ion cannot appreciably change and the energy of relative motion cannot be strongly transferred to another degrees of freedom during the short reaction time.

The interaction energy between ions is obtained with the help of a local energy density functional. The extended Thomas–Fermi (ETF) approximation with $\hbar^2$ correction terms is used for the evaluation of the kinetic energy density functional [9]. The Skyrme and Coulomb energy density functionals are employed for the calculation of the potential energy. These energy density functionals depend on the proton and neutron densities. These densities are obtained in the microscopic Hartree–Fock–Bogoliubov approximation with the Skyrme force. Our approximation is semi-microscopic because we use the microscopic density distributions and the ETF approximation for the calculation of the interaction energy of ions. Note that the binding energies of nuclei evaluated in the ETF approximation with the help of microscopic density distributions well agree with those obtained in the fully microscopic Hartree–Fock–Bogoliubov model [8]. Therefore, our semi-microscopic method for evaluation of the interaction potential between various nuclei is quite accurate.

Unfortunately, the semi-microscopic approach is not so convenient for any practical application because one needs to evaluate the microscopic Hartree–Fock–Bogoliubov densities for both nuclei. Therefore, we choose 119 spherical or near spherical nuclei along the $\beta$-stability line from $^{16}$O to $^{212}$Po and perform calculations of the interaction potentials between all possible nucleus–nucleus combinations in the semi-microscopic approximation. We evaluate potential for any nucleus–nucleus combinations at 15 distances between ions around the touching point. By using database for 7140 ion–ion potentials at 15 points each, we find an analytical expression for the ion–ion potential. The potentials obtained by means of the analytical expression well agree with semi-microscopic one.

In Section 2 of the Letter we briefly discuss our semi-microscopic approach for the ion–ion interaction potential. The simple expression for the nuclear potential between heavy ions is presented in Section 3. The discussion of the results and conclusion are given in Section 4.

## 2. Semi-microscopic potential between heavy ions

The interaction energy between spherical nuclei in the approximation of frozen densities is determined as the difference between binding energy $E_{12}(R)$ at finite distance between ions $R$ and binding energies $E_{1,2}$ of each ion at infinite distance

$$V(R) = E_{12}(R) - E_1 - E_2, \tag{1}$$

where

$$E_{12}(R) = \int \varepsilon\big[\rho_{1p}(\mathbf{r}) + \rho_{2p}(R,\mathbf{r}), \rho_{1n}(\mathbf{r}) + \rho_{2n}(R,\mathbf{r})\big]\,d\mathbf{r}, \tag{2}$$

$$E_1 = \int \varepsilon\big[\rho_{1p}(\mathbf{r}), \rho_{1n}(\mathbf{r})\big]\,d\mathbf{r},$$

$$E_2 = \int \varepsilon\big[\rho_{2p}(\mathbf{r}), \rho_{2n}(\mathbf{r})\big]\,d\mathbf{r}. \tag{3}$$

Here $\varepsilon[\rho_p(\mathbf{r}), \rho_n(\mathbf{r})]$ is the energy density functional, $\rho_{1,2p}(\mathbf{r})$ and $\rho_{1,2n}(\mathbf{r})$ are the proton and neutron density distributions in two interacting spherical nuclei, respectively.

The energy density functional can be presented as a sum of the kinetic $\tau$ and potential $\nu$ parts

$$\varepsilon\big[\rho_p(\mathbf{r}), \rho_n(\mathbf{r})\big] = \frac{\hbar^2}{2m}\big[\tau_p(\mathbf{r}) + \tau_n(\mathbf{r})\big] + \nu(\mathbf{r}), \tag{4}$$

where $m$ is the nucleon mass. Expressions for proton $\tau_p$ and neutron $\tau_n$ kinetic energy density functionals, which take into account $\hbar^2$ correction terms are given in Ref. [9]

$$\begin{aligned}\tau_{p(n)}(\mathbf{r}) = {} & \frac{3}{5}\big(3\pi^2\big)^{2/3}\rho_{p(n)}^{5/3} \\ & + \frac{1}{36}\frac{(\nabla\rho_{p(n)})^2}{\rho_{p(n)}} + \frac{1}{3}\Delta\rho_{p(n)} \\ & + \frac{1}{6}\frac{\nabla\rho_{p(n)}\nabla f_{p(n)} + \rho_{p(n)}\Delta f_{p(n)}}{f_{p(n)}} \\ & - \frac{1}{12}\rho_{p(n)}\left(\frac{\nabla f_{p(n)}}{f_{p(n)}}\right)^2 \\ & + \frac{\rho_{p(n)}}{2}\left(\frac{2m}{\hbar^2}\frac{W_0}{2}\frac{2\nabla\rho_{p(n)} + \nabla\rho_{n(p)}}{f_{p(n)}}\right)^2,\end{aligned} \tag{5}$$

where

$$f_{p(n)}(\mathbf{r}) = 1 + \frac{2m}{\hbar^2}\left(\frac{3t_1 + 5t_2}{16} + \frac{t_2x_2}{4}\right)\rho_{p(n)}(\mathbf{r}). \tag{6}$$

The potential energy density functional splits into nuclear $\nu_{\rm Skyrme}(\mathbf{r})$ and Coulomb $\nu_{\rm Coul}(\mathbf{r})$ parts

$$\nu(\mathbf{r}) = \nu_{\rm Skyrme}(\mathbf{r}) + \nu_{\rm Coul}(\mathbf{r}). \tag{7}$$

The nuclear part is described by the Skyrme energy density functional [9]

$$\begin{aligned}
&\nu_{\rm Skyrme}(\mathbf{r}) \\
&= \frac{t_0}{2}\Big[\big(1+\tfrac{1}{2}x_0\big)\rho^2 - \big(x_0+\tfrac{1}{2}\big)\big(\rho_p^2+\rho_n^2\big)\Big] \\
&\quad + \tfrac{1}{12}t_3\rho^{\alpha}\Big[\big(1+\tfrac{1}{2}x_3\big)\rho^2 - \big(x_3+\tfrac{1}{2}\big)\big(\rho_p^2+\rho_n^2\big)\Big] \\
&\quad + \tfrac{1}{4}\Big[t_1\big(1+\tfrac{1}{2}x_1\big) + t_2\big(1+\tfrac{1}{2}x_2\big)\Big]\tau\rho \\
&\quad + \tfrac{1}{4}\Big[t_2\big(x_2+\tfrac{1}{2}\big) - t_1\big(x_1+\tfrac{1}{2}\big)\Big](\tau_p\rho_p+\tau_n\rho_n) \\
&\quad + \tfrac{1}{16}\Big[3t_1\big(1+\tfrac{1}{2}x_1\big) - t_2\big(1+\tfrac{1}{2}x_2\big)\Big](\nabla\rho)^2 \\
&\quad - \tfrac{1}{16}\Big[3t_1\big(x_1+\tfrac{1}{2}\big) + t_2\big(x_2+\tfrac{1}{2}\big)\Big](\nabla\rho_n)^2 \\
&\quad + (\nabla\rho_p)^2 - \frac{W_0^2}{4}\frac{2m}{\hbar^2}\Big[\frac{\rho_p}{f_p}(2\nabla\rho_p+\nabla\rho_n)^2 \\
&\qquad\qquad + \frac{\rho_n}{f_n}(2\nabla\rho_n+\nabla\rho_p)^2\Big].
\end{aligned} \tag{8}$$

Here and in Eqs. (5), (6), $t_0$, $t_1$, $t_2$, $x_0$, $x_1$, $x_2$, $\alpha$ and $W_0$ are parameters of the Skyrme forces, $\rho = \rho_p + \rho_n$, $\tau = \tau_p + \tau_n$. The last term in Eq. (8) is the spin–orbit interaction obtained in $\hbar^2$ approximation, see Ref. [9] for details.

The Coulomb energy density functional in Eq. (7) is the sum of direct and exchange terms [9]

$$\begin{aligned}
\nu_{\rm Coul}(\mathbf{r}) &= \frac{e^2}{2}\rho_p(\mathbf{r})\int\frac{\rho_p(\mathbf{r}')}{|\mathbf{r}-\mathbf{r}'|}\,d\mathbf{r}' \\
&\quad - \frac{3e^2}{4}\left(\frac{3}{\pi}\right)^{1/3}\big(\rho_p(\mathbf{r})\big)^{4/3}.
\end{aligned} \tag{9}$$

Thus, if we know the proton and neutron density distributions in both nuclei, as well as the gradients and the Laplacians of these distributions, we can calculate the interaction potential between ions by means of the ETF approximation. The nuclear part of interaction potential is evaluated by neglecting the Coulomb interaction between ions at finite distances.

We evaluate the proton and neutron densities in the microscopic Hartree–Fock–Bogoliubov model with SkM* parameter set of the Skyrme force [10]. The pairing is evaluated in Lipkin–Nogami BCS approximation [11]. The monopole pairing constants for protons and neutrons are choosed in the form $G_{p(n)} = 15/(11 + Z(N))$, where $Z$ and $N$ are the number of protons and neutrons in nuclei, respectively. The value of the paring constant for neutrons is the same as in [12], while the proton pairing constant slightly deviates from that evaluated in [12]. We numerically take gradients and Laplacians of density distributions. Note that the semi-microscopic potentials evaluated for different sets of the Skyrme force well agree with each other at distances larger than and near the touching distance [8]. Some sets of the Skyrme force (for example, Sk3) may give essentially different results at distances less than the touching one, when the densities of ions are strongly overlapped [8]. The difference between semi-microscopic ion–ion potentials, evaluated with different sets of the Skyrme force at small distances between ions, is related to different values of incompressibility for these sets. We choose SkM* parameter set of the Skyrme force [10] because the corresponding incompressibility is close to the experimental one [9,13] and this parameter set is successfully applied to the description of various nuclear structure phenomena.

## 3. Analytical expression for potential between heavy ions

We choose 119 spherical or near spherical even-even nuclei around the $\beta$-stability line from $^{16}$O to $^{212}$Po and perform calculations of the nuclear part of interaction potentials in the semi-microscopic approximation between all possible nucleus–nucleus combinations. Therefore, we evaluate 7140 ion–ion potentials at 15 distances around the touching point. By using this database we find expression for the nuclear part of ion–ion interaction potential in the form

$$\begin{aligned}
V(R) &= -1.989843Cf(R - R_{12} - 2.65) \\
&\quad \times \big[1 + 0.003525139(A_1/A_2 + A_2/A_1)^{3/2} \\
&\quad - 0.4113263(I_1 + I_2)\big],
\end{aligned} \tag{10}$$

where $R$ is the distance between mass centers of colliding nuclei, $C = R_1R_2/R_{12}$, $R_i$ is the effective

nuclear radius, $R_{12} = R_1 + R_2$,

$$f(s) = \left\{1 - s^2\left[0.05410106C\exp\left(-\frac{s}{1.760580}\right) - 0.5395420(I_1 + I_2)\exp\left(-\frac{s}{2.424408}\right)\right]\right\} \times \exp\left(\frac{-s}{0.7881663}\right), \quad \text{for } s \geqslant 0, \tag{11}$$

$$f(s) = 1 - \frac{s}{0.7881663} + 1.229218s^2 - 0.2234277s^3 - 0.1038769s^4 - C\left(0.1844935s^2 + 0.07570101s^3\right) + (I_1 + I_2)\left(0.04470645s^2 + 0.03346870s^3\right), \quad \text{for } -5.65 \leqslant s \leqslant 0, \tag{12}$$

$A_i$ is the number of nucleon in nucleus $i$ ($i = 1, 2$), $I_i = (N_i - Z_i)/A_i$, $Z_i$ and $N_i$ are numbers of protons and neutrons in nucleus $i$. The effective nuclear radius is given by

$$R_i = R_{ip}\left(1 - 3.413817/R_{1p}^2\right) + 1.284589\left(I_i - 0.4A_i/(A_i + 200)\right), \tag{13}$$

where the proton radius is determined as in [14]

$$R_{ip} = 1.24A_i^{1/3}(1 + 1.646/A_i - 0.191I_i). \tag{14}$$

The last term in (13) takes into account deviation of the nuclear radius from the proton radius when the neutron number in nucleus deviates from the $\beta$-stability value for given $A$. The line of $\beta$-stability is described by Green's approximation $I = (N - Z)/A = 0.4A/(A + 200)$ [15].

Each nucleus–nucleus potential is evaluated at the 15 distances between ions, which are determinated as

$$D_k = R_{1p} + R_{2p} + 0.5(k - 7)\ \text{fm}, \quad \text{where } k = 1, 2, 3, \ldots, 15. \tag{15}$$

The parameters and the form of Eqs. (10)–(13) are found by the minimization of

$$\sum_{n=1}^{7140}\sum_{k=1}^{15}\frac{(V_n(D_k) - V_n^{s-m}(D_k))^2}{-V_n^{s-m}(D_k)}, \tag{16}$$

where $V_n^{s-m}(D_k)$ is the potential evaluated in the semi-microscopic approximation and $V_n(D_k)$ is the potential described by the analytical approximation. For a more accurate description of the potential at large distances, where the potential is rather small, we use the weight $-1/V_n^{s-m}(D_k)$ in (16). (Please, remember that $V_n^{s-m}(D_k)$ is negative.)

Table 1
Dependence of rms error $\delta(D_k)$ (13) on distance $D_k$ (11) between ions

| $k$ | 1 | 2 | 3 | 4 | 5 |
|---|---|---|---|---|---|
| $\delta(D_k)$, MeV | 2.15 | 1.63 | 1.01 | 0.90 | 0.80 |
| $k$ | 6 | 7 | 8 | 9 | 10 |
| $\delta(D_k)$, MeV | 0.64 | 0.58 | 0.43 | 0.27 | 0.18 |
| $k$ | 11 | 12 | 13 | 14 | 15 |
| $\delta(D_k)$, MeV | 0.10 | 0.060 | 0.041 | 0.028 | 0.020 |

The root mean square error (rms error)

$$\delta(D_k) = \left(\frac{1}{7140}\sum_{n=1}^{7140}\left(V_n(D_k) - V_n^{s-m}(D_k)\right)^2\right)^{1/2} \tag{17}$$

is presented in Table 1. The barrier formed by Coulomb and nuclear interactions between ions takes place, as a rule, at distances between $D_9$ and $D_{13}$. So, by using the analytical expression for the potential we may estimate the barrier with rms error smaller then 0.3 MeV, see Table 1.

The main goal of this study is to present a simple expression for the nuclear interaction potential between ions at distances around the touching point, which is suitable for determination of the barrier and the shape of potential well (pocket). The rms error is small for such distances, see Table 1. Note that the rms error is relatively large (compared to the potential value) for a large distances between ions like $D_{15}$, but the nuclear part of ion–ion potential is rather small for such distances.

## 4. Discussion and conclusion

As, an example, in Fig. 1 we compare the nuclear part of the ion–ion potential near touching point obtained in our approach with other potentials available in Refs. [1,4–7] for all different nucleus–nucleus combinations of $^{16}$O, $^{90}$Zr and $^{208}$Pb.

Semi-microscopic potentials are well fitted by our analytical expression, see Fig. 1. However, for some cases the agreement at small distances is worse then at the larger ones. This tendency also reveals itself in Table 1. In Fig. 1 we see that Krappe–Nix–Sierk

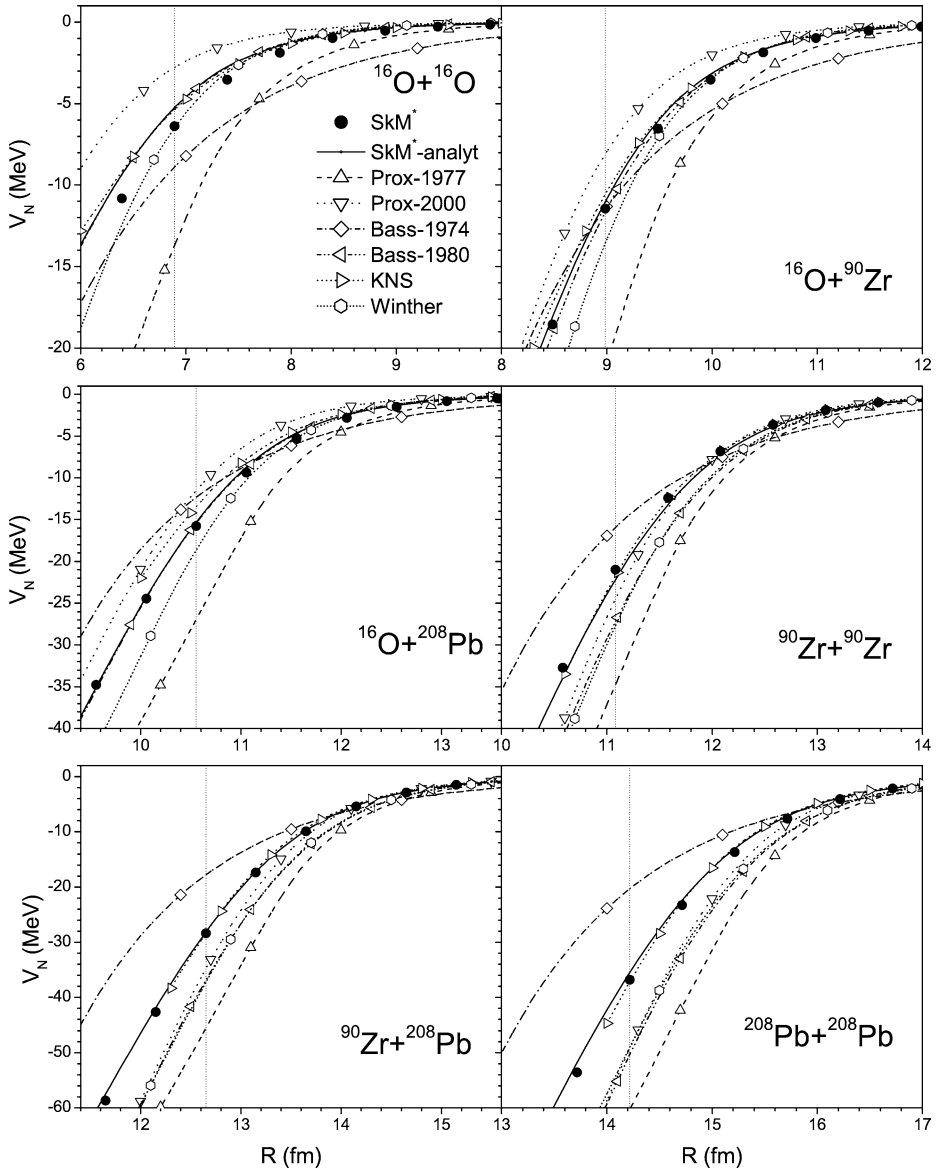


Fig. 1. The nuclear part of the ion–ion potential for reactions $^{16}\mathrm{O}+{}^{16}\mathrm{O}$, $^{16}\mathrm{O}+{}^{90}\mathrm{Zr}$, $^{16}\mathrm{O}+{}^{208}\mathrm{Pb}$, $^{90}\mathrm{Zr}+{}^{90}\mathrm{Zr}$, $^{90}\mathrm{Zr}+{}^{208}\mathrm{Pb}$ and $^{208}\mathrm{Pb}+{}^{208}\mathrm{Pb}$. The potential obtained in direct semi-microscopic calculations is marked by dots, the potential obtained by using analytical expressions (10)–(14) is shown by the solid line. The touching point distance of two ions ($D_7$) is marked by the vertical dotted line on each figure.

[5] potential is the closest to that in our approach. Unfortunately, this potential is introduced only up to the touching distance of ions [5]. The proximity-2000 potential was also originally derived up to the touching distance [6], but in the Fig. 1 we slightly extrapolate it to smaller distances by using analytical expression for proximity-2000 potential given in [6].

In Fig. 1 we see that the proximity-1977 potential [4] is the most attractive at large distances. The Bass-1974 (Eqs. (7.37)–(7.39) in Ref. [1]) potential is the weakest potential at large distances for

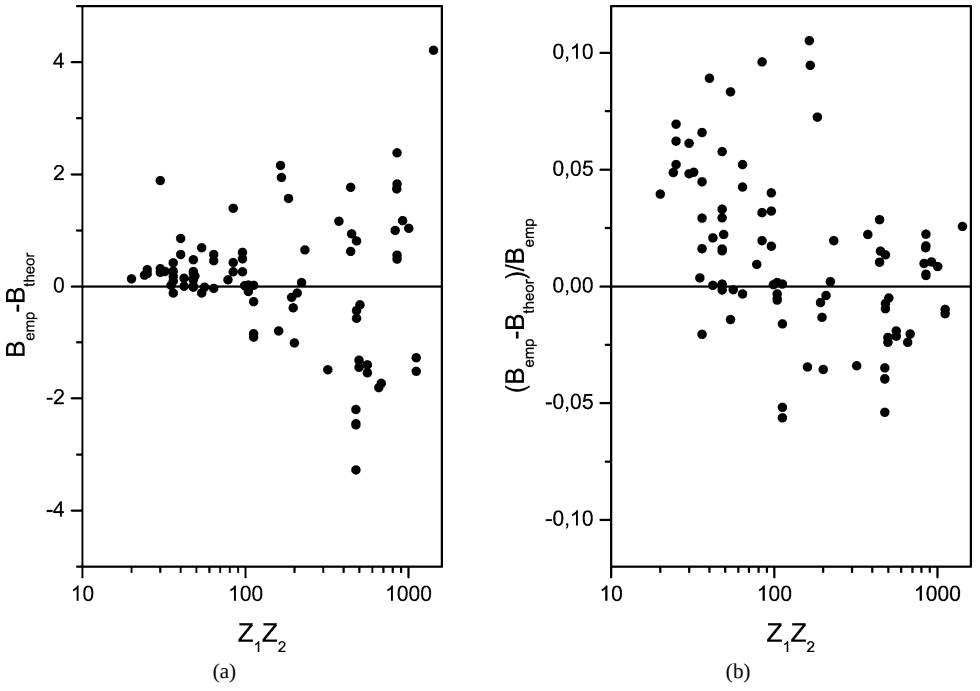


Fig. 2. The difference between the "empirical fusion barrier" and the barrier evaluated with expressions (10)–(14).

medium and heavy systems. Due to different $A$- and $Z$-dependencies, the proximity-1977 [4], proximity-2000 [6], Krappe–Nix–Sierk [5], Bass-1974 [1], Bass-1980 (Eqs. (7.50), (7.51) in Ref. [1]), Winther [7] and our analytical potentials have different mutual positions for different systems in Fig. 1. For example, we see that Bass-1980 potential is close to semi-microscopic potential for light systems, while the Bass-1980 potential becomes more attractive than the semi-microscopic one for heavier systems. Proximity-1977 [4], proximity-2000 [6], Bass-1980 [1] and Winther [7] potentials are overattractive for very heavy colliding systems. Due to this, the barriers evaluated with these potentials are too low as compared to our predictions. The knowledge of the interaction barrier is very important for the correct understanding of the superheavy element production mechanism [6,8,16,17] and subbarrier fusion of medium-weight nuclei [18]. (Note that exact calculation of the Coulomb interaction energy between very heavy nuclei is necessary for the accurate evaluation of the interaction potential around touching points because the Coulomb energy evaluated in the approximation of two point-like ions results in considerably less of accuracy in such cases.)

The "empirical fusion barrier" $B_{\rm emp}$ between heavy ions is extracted by means of a special analysis of the experimental data for subbarrier fusion reactions in Ref. [19]. The difference between "empirical fusion barrier" and barrier evaluated by using expressions (10)–(14) $B_{\rm theor}$ is presented in Fig. 2. The barriers $B_{\rm theor}$ well agree with "empirical fusion barriers", see Fig. 2. Note that "empirical fusion barrier" is determined with the accuracy[1] $\pm 2\%$ for $Z_1Z_2 \lesssim 800$ and $\pm 3$–$8\%$ for $Z_1Z_2 \gtrsim 800$ [19].

The distribution of deviations $B_{\rm emp} - B_{\rm theor}$ is almost symmetric with respect to the line $B_{\rm emp} - B_{\rm theor} = 0$, see Fig. 2. This also suggests the reliability of

[1] The accuracy of the "empirical fusion barrier" is worse then that given in [19], because the model used for description of experimental fusion cross section in Ref. [19] is oversimplified. It is well-known that the coupling to both low-energy surface vibrations and nucleon transfer between ions strongly enhances the subbarrier fusion cross section [16–18,20]. These effects are not considered in the "empirical fusion barrier" evaluation in Ref. [19].

$A$- and $Z$-dependencies of our approach. In contrast similar distributions for the proximity-1977, proximity-2000 and Krappe–Nix–Sierk potentials have no symmetry with respect to the line $B_{\mathrm{emp}}-B_{\mathrm{theor}}=0$, see Fig. 5 in Ref. [19] and Figs. 1 and 2 in Ref. [6].

The potential described by Eqs. (10)–(14) well agrees with the semi-microscopic the one for all systems in Fig. 1. So, the results presented in Table 1 and in Figs. 1 and 2 suggest that the $A$- and $Z$-dependencies of the nuclear ion–ion potential described by Eqs. (10)–(14) are the most realistic.

## Acknowledgements

The author would like to thank W. Nörenberg, Yu. Ivanov, P. Rozmej and D. Voskresensky for useful discussions and help. The author gratefully acknowledges support from GSI.

## References

[1] R. Bass, Nuclear Reactions with Heavy Ions, Springer-Verlag, Berlin, 1980.
[2] P.E. Hodgson, Nuclear Heavy-Ion Reactions, Clarendon Press, Oxford, 1978.
[3] W. Nörenberg, H.A. Weidenmüller, Introduction to the Theory of Heavy-Ion Collisions, Springer-Verlag, Berlin, 1980.
[4] J. Blocki, J. Randrup, W.J. Swiatecki, C.F. Tang, Ann. Phys. (N.Y.) 105 (1977) 427.
[5] H.J. Krappe, J.R. Nix, A.J. Sierk, Phys. Rev. C 20 (1979) 992.
[6] W.D. Myers, W.J. Swiatecki, Phys. Rev. C 62 (2000) 044610.
[7] A. Winther, Nucl. Phys. A 594 (1995) 203.
[8] V. Yu. Denisov, W. Nörenberg, in preparation.
[9] M. Brack, C. Guet, H.-B. Hakanson, Phys. Rep. 123 (1985) 275;
M. Brack, R.K. Bhaduri, Semiclassical Physics, Addison–Wesley, Reading, MA, 1997.
[10] J. Bartel, Ph. Quentin, M. Brack, C. Guet, H.-B. Hakansson, Nucl. Phys. A 386 (1982) 79.
[11] H.J. Lipkin, Ann. Phys. 31 (1960) 525;
Y. Nogami, Phys. Rev. 134 (1964) B313;
H.C. Pradhan, Y. Nogami, J. Law, Nucl. Phys. A 201 (1973) 357.
[12] L. Bennour, P.-H. Heenen, P. Bonche, J. Dobaczewski, H. Flocard, Phys. Rev. C 40 (1989) 2834.
[13] J.-P. Blaizot, Phys. Rep. 64 (1980) 171.
[14] B. Nerlo-Pomorska, K. Pomorski, Z. Phys. A 348 (1994) 169.
[15] A.E.S. Green, Nuclear Physics, McGraw–Hill, New York, 1955.
[16] V.Yu. Denisov, S. Hofmann, Phys. Rev. 61 (2000) 034606;
V.Yu. Denisov, S. Hofmann, Acta Phys. Pol. B 31 (2000) 479.
[17] V.Yu. Denisov, in: Proc. Tours Symposium on Nuclear Physics IV, Tours France, September, 2000, AIP Conf. Proc., Vol. 561, 2001, p. 433;
V.Yu. Denisov, in: Proc. Int. Workshop on Fusion Dynamics at the Extremes, Dubna, May, 2000, World Scientific, Singapore, 2001, p. 203;
V.Yu. Denisov, Prog. Part. Nucl. Phys. 46 (2001) 303.
[18] V.Yu. Denisov, Phys. At. Nucl. 62 (1999) 1349;
V.Yu. Denisov, Eur. Phys. J. A 7 (2000) 87.
[19] L.C. Vaz, J.M. Alexander, G.R. Sachler, Phys. Rep. 69 (1981) 373.
[20] M. Beckerman, Phys. Rep. 129 (1985) 145;
W. Reisdorf, J. Phys. G 20 (1994) 1297;
M. Dasgupta, D.J. Hinde, N. Rowley, A.M. Stefanini, Annu. Rev. Nucl. Part. Sci. 48 (1998) 401.